

Inhibited biofilm formation and improved antibacterial activity of a novel nanoemulsion against cariogenic *Streptococcus mutans* in vitro and in vivo

Yun Fei Li,^{1,2,*} Hong Wu Sun,^{1,2,*}
Rong Gao,^{1-3,*} Kai Yun Liu,^{1,2} Hua
Qi Zhang,⁴ Qi Huan Fu,^{1,2} Sheng Li
Qing,^{1,2} Gang Guo,^{1,2} Quan Ming
Zou^{1,2,*}

¹National Engineering Research Center of Immunological Products, ²Department of Microbiology and Biochemical Pharmacy, College of Pharmacy, ³Department of Biomedical Engineering, Third Military Medical University of Chinese PLA, Chongqing, People's Republic of China; ⁴Wanzhou Institute for Food and Drug Control of Chongqing, Wanzhou, Chongqing, People's Republic of China

*These authors contributed equally to this work

→ Video abstract



Point your SmartPhone at the code above. If you have a QR code reader the video abstract will appear. Or use:

<http://dxpr.es/1CH44uT>

Correspondence: Hong Wu Sun; Quan Ming Zou
National Engineering Research Center for Immunological Products and Department of Microbiology and Biochemical Pharmacy, College of Pharmacy, Third Military Medical University of Chinese PLA, 30 Sha Ping Ba Gaotanyan Street, Chongqing, 400038, People's Republic of China
Tel +86 023 6875 2377
Fax +86 023 6875 2377
Email sunhongwu2001@163.com; qmzou2007@163.com

Abstract: The aim of this study was to prepare a novel nanoemulsion loaded with poorly water-soluble chlorhexidine acetate (CNE) to improve its solubility, and specifically enhance the antimicrobial activity against *Streptococcus mutans* in vitro and in vivo. In this study, a novel CNE nanoemulsion with an average size of 63.13 nm and zeta potential of -67.13 mV comprising 0.5% CNE, 19.2% Tween 80, 4.8% propylene glycol, and 6% isopropyl myristate was prepared by the phase inversion method. Important characteristics such as the content, size, zeta potential, and pH value of CNE did not change markedly, stored at room temperature for 1 year. Also, compared with chlorhexidine acetate water solution (CHX), the release profile results show that the CNE has visibly delayed releasing effect in both phosphate-buffered saline and artificial saliva solutions ($P < 0.005$). The minimum inhibitory concentration and minimum bactericidal concentration of CHX for *S. mutans* (both 0.8 $\mu\text{g}/\text{mL}$) are both two times those of CNE (0.4 $\mu\text{g}/\text{mL}$). Besides, CNE of 0.8 $\mu\text{g}/\text{mL}$ exhibited fast-acting bactericidal efficacy against *S. mutans*, causing 95.07% death within 5 minutes, compared to CHX (73.33%) ($P < 0.01$). We observed that 5 mg/mL and 2 mg/mL CNE were both superior to CHX, significantly reducing oral *S. mutans* numbers and reducing the severity of carious lesions in Sprague Dawley rats ($P < 0.05$), in an in vivo test. CNE treatment at a concentration of 0.2 $\mu\text{g}/\text{mL}$ inhibited biofilm formation more effectively than CHX, as indicated by the crystal violet staining method, scanning electron microscopy, and atomic force microscopy. The cell membrane of *S. mutans* was also severely disrupted by 0.2 $\mu\text{g}/\text{mL}$ CNE, as indicated by transmission electron microscopy. These results demonstrated that CNE greatly improved the solubility and antimicrobial activity of this agent against *S. mutans* both in vitro and in vivo. This novel nanoemulsion is a promising medicine for preventing and curing dental caries.

Keywords: nanoemulsion, chlorhexidine acetate, *Streptococcus mutans*, antibacterial

Introduction

Dental caries can cause pain, infection, and tooth loss, negatively affecting eating, speaking, and general health.¹ Poor oral health and tooth loss have been considered as possible risk factors for some chronic diseases, including gastric cancer.² Dental caries represent a major public health problem globally, and 95% of the world population (approximately 5 billion people) currently have cavities. The World Health Organization reports that 60%–90% of school children worldwide have experienced caries, with the disease being most prevalent in Asia and Latin American countries.³ In the People's Republic of China, the prevalence of dental caries in the elderly population in different regions ranges from 66.03% to 87.42% in 2009–2013.⁴ The prevalence

of caries among children was 84.3%, and the prevalence of incipient caries lesion was 50.8%.⁵ This global increase in the prevalence of dental caries also affects adults. This increase in dental caries signals an impending public health crisis.⁶

Streptococcus mutans has been implicated as the primary etiological agent of dental caries and plays a critical role in dental plaque biofilm formation and the development of dental caries.⁷ The inhibition of *S. mutans* is essential for the successful control and prevention of dental caries. The antibacterial compounds used in tooth pastes and mouth rinses include povidone-iodine, chlorhexidine digluconate,⁸ cetylpyridinium chloride, triclosan, zinc citrate, fluorides, and other antimicrobial substances that effectively inhibit *S. mutans*. However, these substances may cause undesirable effects, such as vomiting, diarrhea, and tooth staining. Chlorhexidine acetate (CNE), which is known as a chemical antiseptic, has been found to exhibit antimicrobial activity against dental pathogens in many studies.⁹ In addition, chlorhexidine varnish exhibited better efficacy than fluoride varnish in an in vivo study.¹⁰ We believe that CNE is a promising drug for caries. However, it is rarely used in a mouthwash because of its limited water solubility.¹¹

A nanoemulsion is an emulsion with a droplet size ranging from 1 to 100 nm. Nanoemulsions can be widely used for drug delivery due to their extremely small size, their biocompatibility, their relative stability, and their abilities to solubilize large quantities of hydrophobic compounds, change drug odor, and protect drugs from hydrolysis under physiological conditions.¹² No reports concerning CNE nanoemulsions are currently available. In this study, we prepared a novel nanoemulsion loaded with poorly water-soluble CNE and aimed to improve the solubility of this compound and enhance its therapeutic efficacy against cariogenic *S. mutans* in vivo and in vitro. Minimum inhibitory concentration (MIC) and minimum bactericidal concentration (MBC) of CNE and chlorhexidine acetate water solution (CHX) against *S. mutans* were first determined. In addition, the action mechanism of this compound in the context of biofilm formation and the structure and integrity of the cell membrane were studied using scanning electron microscopy (SEM), atomic force microscopy (AFM), and transmission electron microscopy (TEM).

Materials and methods

Bacterial strains and growth conditions

S. mutans strain UA159 (American Type Culture Collection [ATCC] 700610) was purchased from the ATCC (Manassas, VA, USA). Brain heart infusion (BHI) (BD, Franklin Lakes, NJ, USA) was used for bacterial culture. Bacterial stocks were maintained at -80°C in BHI containing 30% (v/v)

glycerol. Aliquots of the stock culture were inoculated into fresh BHI and cultured in 10% H_2 , 5% CO_2 , and 85% N_2 overnight at 37°C . Bacterial cultures with an optical density (OD) at 595 nm of 1.0, which represented 1×10^9 colony forming units (CFU/mL), were used for all studies.

Preparation of the novel CNE nanoemulsion

The nanoemulsion composition was screened based on CNE (Jinzhou Jiutai Pharmaceutical Co., Ltd, Liaoning, People's Republic of China; CP2010, 98.3%) solubility in five types of oil phases (ie, IPM [isopropyl myristate; Croda, Goole, UK], GTCC [caprylic/capric triglyceride; Beijing Fengli Pharmaceutical Co., Ltd, Beijing, People's Republic of China], liquid paraffin, peanut oil, and soybean oil), five types of cosurfactants (ie, ethyl, propylene glycol, glycerin, Span 80, Span 85), and five types of surfactants (ie, Tween 80, Tween 85, Tween 20, RH 40 [Cremophor RH 40; BASF, Mumbai, India], and EL 40 [Cremophor EL 40; BASF, Mumbai, India]). Briefly, an excess amount of CNE was added into tubes of each agent described above and then vortex-mixed for about 1 minute. The tubes were shaken continually at room temperature for 24 hours, followed by equilibrium for 24 hours. The mixture was then centrifuged at $13,000 \times g$ for 10 minutes to obtain a clear solution and then was diluted with methanol and analyzed by HPLC (high-performance liquid chromatography). The solubility was determined by ultraviolet-visible detector integrated with Alliance HPLC (Waters®, E2695; Waters, MA, USA) and operated with ZORBAX SB-C18 Chromolith HPLC column (5 μm , 4.6 mm \times 250 mm). At a flow rate of 1.0 mL/min, elution was conducted using a mobile phase of acetonitrile/0.02 M K_2HPO_4 (pH=2.0) (70/30, v/v), and detection was monitored at a wavelength of 275 nm with 10 μL injection volume at room temperature. We chose the higher solubility of CHX in oil phase, surfactant, and cosurfactant as nanoemulsion formula. On the basis of a preliminary solubility experiment, we chose IPM as the oil phase, Tween 80 as the surfactant, propylene glycol as the cosurfactant, and water as the aqueous phase for this study. A novel nanoemulsion formula was prepared, as described previously.¹³ Briefly, a powder of CNE was added to the mixture of Tween 80, propylene glycol, and IPM, and the nanoemulsion was prepared by phase inversion method, adding the mixture dropwise to the aqueous phase under gentle agitation until a transparent and easily flowing nanoemulsion was observed.

Physicochemical characterization of CNE

Morphological characterization: CNE was diluted 50 times with distilled water, placed on a carbon-coated copper

grid, and covered with a drop of 1% phosphotungstic acid (pH 7.4). Excess phosphotungstic acid was removed with a filter paper. Images were obtained using a TECNAI-10 TEM (Philips, Amsterdam, Holland). Combinations of bright-field images captured using increased magnification and diffraction modes were utilized to reveal the form and particle size of this nanoemulsion.

Size distribution, zeta potential, and physicochemical data: CNE was diluted 50 times with distilled water and the diameter was measured via dynamic light scattering using a Malvern Zetasizer Nano ZS90 photon correlation spectroscope (Malvern Instruments, Malvern, UK) at 633 nm. The scattering intensity was measured at a scattering angle of 173° relative to the source using a cascade of photodiode detectors at 25°C. Intensity autocorrelation functions were analyzed using general purpose algorithm software (Malvern Zetasizer) to determine the distribution of the translational Z-averaged diffusion coefficients of the particles. In addition, basic CNE physical characteristics, including the polydispersity index (PDI), zeta potential, viscosity, and refractive index (RI), were also determined using previously described methods.

Stability assessment of CNE

High-speed centrifuge test

The thermodynamic stability of CNE was evaluated after centrifugation for 30 minutes at 13,000× *g* and 25°C. The appearance of these formulations was investigated using indexes such as turbidity, phase separation, precipitation, drug separation, demulsification, and creaming.¹³

Long stability test

In accordance with the Technical Standard of Drug Stability Test¹⁴, stability studies were carried out for CNE. Importantly, drug content, size, zeta potential, and pH values were chosen as markers for stability evaluation in this study. For the stability test, samples were filled in amber-colored containers with nitrogen gas protection and stored at room temperature for a year. Samples were withdrawn at time intervals of 0, 30, 60, 90, 180 and 360 days. After that, the samples were centrifuged at 13,000× *g* for 10 minutes to remove the precipitated CHX, if any. CHX content in the supernatant liquid was determined using the above described HPLC methods. Size and zeta potential of all samples were measured by laser scattering with Nano ZS90 at room temperature. pH values of each sample were tested by a pH meter (Sartorius PB-10, Sartorius AG, Göttingen, Germany).

In vitro release studies

In order to optimize drug delivery and achieve an ideal therapeutic effect, we incorporated the drug with nanoemulsion droplets for intraoral use. Therefore, it was extremely important to observe the release of CHX from the nanoemulsions in comparison with that of the drug in phosphate-buffered saline (PBS) and artificial saliva. In vitro release studies were performed in 200 mL of artificial saliva¹⁵ (ISO/TR10271 standard, sodium chloride [0.4 g/L], calcium chloride dihydrate [0.795 g/L], potassium chloride [0.4 g/L], sodium sulfide dihydrate [0.005 g/L], sodium dihydrogen phosphate [0.78 g], and urea [1 g/L], pH 6.8) and PBS (0.1 M, pH 6.8) as a release medium. The test bags were soaked in release medium at a stirring rate of 100 rpm at room temperature. Approximately 2 mL sample of 0.5% CNE and 0.5% CHX suspension was placed in a treated dialysis bag (SP132574, Molecular Weight Cut Off 10,000 g/mol; Sangon Biotech (Shanghai) Co., Ltd, Shanghai, People's Republic of China). Approximately 0.2 mL samples were removed at regular time intervals at 0, 0.25, 0.5, 0.75, 1, 1.5, 2, 3, 4, 6, 8, 10, and 12 hours. Meanwhile, the same volume of fresh release medium was added to maintain the same volume. The sample solution was centrifuged at 10,000× *g* for 10 minutes and the supernatant liquid was measured using the HPLC methods described above.

Determination of MIC and MBC

According to the modified method¹⁶ and the results of the preliminary experiment with a series of tenfold dilution, CNE and CHX were individually diluted to 1, 2, 4, 8, and 16 µg/mL of CNE with distilled water. Then, 0.2 mL solutions were individually added to 1.8 mL of BHI bacterial suspension (10⁷ CFU/mL) and incubated anaerobically (Thermo 3427; Thermo Scientific, Waltham, MA, USA) in 24-well plates (Costar 3524; Corning Inc., Corning, NY, USA) at 37°C for 24 hours, with shaking at 200× *g*. After incubation, 200 µL samples from each well were moved to a 96-well plate and tested using an enzyme-linked immunosorbent reader (BioRad 6.0; Bio-Rad Laboratories Inc., Hercules, CA, USA) at 595 nm. The highest dilution at which no bacterial growth was detected was recognized as the MIC. Suspension of each concentration group was collected and centrifuged (6,000× *g*, 10 minutes). The precipitate was treated with 0.2 mL of sterilized saline. Then, 5 µL solutions were added to BHI agar plates and incubated at 37°C for 24 hours for MBC test. The highest dilution at which there was no bacterial growth on BHI plates was identified as the MBC. Blank nanoemulsion (BNE) without CNE was diluted at the same time to the highest concentration of CNE as the blank controls.

Time-kill assays

Bacterial cultures (1×10^7 CFU/mL) were incubated for 0, 5, 10, 15, 30, 60, 120, 240, 480, and 720 minutes in CNE and CHX at CNE concentrations of 0.2, 0.4, and 0.8 $\mu\text{g/mL}$ for the killing time assay. After incubation, 5 μL samples were tenfold diluted (10^0 , 10^1 , 10^2 , 10^3 , and 10^4) with BHI culture medium, added to BHI plates, and incubated at 37°C for 24 hours. The number of bacteria on each plate was counted using an auto colony counter (Shineso Science & Technology Co., Ltd, Hangzhou, People's Republic of China). BNE was diluted at the same time to the highest concentration of CNE as blank controls.

Assay for antimicrobial activity of CNE in vivo

Animals

A total of 60 female Sprague Dawley rats (three weeks old, specific pathogen-free) were purchased from the Chongqing Institute of Chinese Medicine (Chongqing, People's Republic of China). The rats were divided into six groups and maintained in specific pathogen-free laboratory conditions (room temperature, $23^\circ\text{C} \pm 2^\circ\text{C}$; relative humidity, $55\% \pm 5\%$; 12-hour light, 12-hour dark cycle) with free access to autoclaved pellet-fed Keys Diet 2000 and sterile water.

Animal study

Animal experiments were approved by the Animal Ethical and Experimental Committee of Third Military Medical University in Chongqing, People's Republic of China. Following the identification of *S. mutans* in the oral cavity, antibiotic solutions in water (ie, 1% chloramphenicol, 1% ampicillin, and 1% carbenicillin [w/w]) were administered orally for 3 days. Bacterial suspensions were set at a concentration of 1.0×10^9 CFU/mL. All groups of rats were orally inoculated with 0.2 mL of bacterial suspensions via gavage daily for 3 days. All rats except the model control group (Group 6) were treated orally for 28 days with 0.2 mL of suspension for 30 seconds twice daily as follows: Group 1, 2 mg/mL of CHX (0.2%); Group 2, 5 mg/mL of chlorhexidine acetate water suspension solution (0.5% CHX); Group 3, 2 mg/mL of CNE nanoemulsion (0.2% CNE); Group 4, 5 mg/mL of CNE nanoemulsion (0.5% CNE); Group 5, BNE control. After treatment for 14 and 28 days, 5 μL oral samples were diluted 100 times with sterilized saline, added to Mitis Salivarius agar plates (BD), and incubated at 37°C for 72 hours to isolate *S. mutans*. The number of bacteria on each plate was counted using an auto colony counter

(Shineso Science & Technology Co., Ltd). The experiment lasted for 70 days, and all animals were euthanized by CO_2 asphyxiation. The left and right jaws were defleshed, and the teeth were prepared for caries scoring. Caries on the smooth and sulcal surfaces and their severity (E, Enamel; Ds, dentin exposed; Dm, $\frac{3}{4}$ of dentin affected) were evaluated using the Keyes scoring system.^{17–18}

Inhibition of biofilm formations by CNE

Quantification of biofilm formation

Biofilm formation was assessed as previously described by Krzysciak with some modifications.¹⁹ About 1.8 mL portions of an overnight broth culture containing *S. mutans* strains (10^6 CFU/mL) were added to each well of 24-well tissue culture plates and treated individually with 0.2 mL of CNE and CHX (with 0.2 $\mu\text{g/mL}$ of CNE). The plates were incubated aerobically for 48 hours. The supernatant was subsequently removed, and the wells were gently washed twice with sterilized distilled water. Attached bacteria were fixed with 1 mL of methanol per well for 15 minutes. The microplates were subsequently emptied and air dried. Each well was stained for 15 minutes with 0.2 mL of 0.1% (w/w) crystal violet. Excess stain was rinsed off by placing the microplates under running tap water. The microplates were air dried, and the dye bound to the adherent cells was removed with 0.2 mL of 30% (v/v) glacial acetic acid per well. The OD of the resulting solutions was read at 595 nm using a microplate reader.

Observation of surface structures of biofilm formation by SEM

A 1.8 mL portion of an overnight broth culture containing *S. mutans* strains (10^6 CFU/mL) was added to each well of 24-well tissue culture plates and subsequently treated individually with 0.2 mL of CNE and CHX (with 0.2 $\mu\text{g/mL}$ of CNE). Coverslips (Thermo, Rochester, NY, USA) were previously placed in each well. The plates were incubated aerobically for 48 hours. After withdrawing the supernatant medium, the biofilms were air dried and treated overnight with 2 mL of 2.5% glutaraldehyde solution for fixation. After fixation, the biofilms were dehydrated in a graded series (ie, 10%, 30%, 50%, 70%, 90%, and 100%) of ethanol and a graded series (ie, 10%, 30%, 50%, 70%, 90%, and 100%) of isobutyl alcohol. Instead of a critical point dryer, the biofilms were treated with 100% hexamethyldisilazane for 10 minutes and coated with gold. The specimens were observed by a scanning electron microscope (AMRAY1000 B; Amray Inc., Bedford, MA, USA).

Observation of three-dimensional structures of biofilm formation by AFM

All coverslips for evaluating biofilm formation were treated as above for methods similar to scanning electron microscopy. The coverslips were air dried after removing the supernatant medium. A high-resolution atomic force microscope (IPC-208B; Chongqing University, Chongqing, People's Republic of China) was utilized to characterize the molecular morphology of the biofilm. The coverslips were tested after washing twice with sterilized distilled water. Measurements were obtained under the following conditions: tungsten probes (force constant, 0.06 N·m); scan range, 1,232 nm × 1,232 nm; imaging mode, tapping mode; and the scanning method, point-by-point scanning at room temperature. Three profile parameters, roughness average (R_a), mean roughness depth (R_z), and mean square roughness (R_q), and the measure parameters skewness (R_{sk}) and Kurtosis (R_{ku}) were calculated by the G3DR software (Chongqing, People's Republic of China).

Cell membrane damage by CNE

Cell membrane structural damage

All samples were treated using biofilm formation methods described above. After centrifuging, the cells were washed twice with 0.1 M PBS and fixed with 2.5% (v/v) glutaraldehyde in 0.1 M PBS. The samples were postfixed with 2% (w/v) OSO_4 in 0.1 M PBS for 1 hour at room temperature and washed three times with the same buffer, then dehydrated in a series of ethanol solutions (ie, 50%, 70%, 80%, 90%, 95%, and 100%). Each specimen was embedded in a spur resin and cut using a ultracut ultramicrotome (SuperNova; Reichert-Jung Optische Werke, Vienna, Austria), stained using uranyl acetate and alkaline lead citrate, and observed using TECNAI-10 TEM.

Integrity of the cell membrane

The cell membrane integrity of *S. mutans* was determined by the release of DNA and protein which was detected with absorption value at 260 and 280 nm. Bacterium fluid (1×10^6 CFU/mL) was incubated in 24-well culture plates for 4 hours with CNE and CHX at 0.2, 0.4, and 0.8 μ g/mL concentrations to assess cell membrane integrity. The OD value of 5 μ L samples that had been centrifuged at $6,000 \times g$ for 10 minutes and dissolved in 0.2 mL of sterilized saline was read using a nano-drop UV-Vis spectrophotometer (ND1000; Thermo Fisher Scientific Inc., Wilmington, DE, USA) at wavelengths of 260 nm and 280 nm.

Statistical analysis

Each experiment was performed with three replicates of the same concentration, for individual microorganisms, except

MIC duplications. The mean of three values was used to calculate the means \pm standard deviations. Statistically significant differences between groups were identified by a P -value of <0.05 . All data were multiple compared using a one-way analysis of variance and analyzed using the SPSS 19.0 statistical software for Windows.

Results

Preparation of the novel CNE nanoemulsion

The solubilities of CHX in the five types of surfactants, Tween 80, RH40, EL40, Tween 85, and Tween 20 are 8.45 ± 0.08 mg/g, 13.23 ± 0.56 mg/g, 10.28 ± 0.17 mg/g, 8.45 ± 0.08 mg/g, and 4.23 ± 0.06 mg/g, respectively. The solubility in different cosurfactants, ethyl alcohol, propylene glycol, glycerin, Span 80, and Span 85 are 9.60 ± 0.31 mg/g, 7.73 ± 0.30 mg/g, 2.09 ± 0.46 mg/g, 3.95 ± 0.03 mg/g, and 4.35 ± 0.11 mg/g, respectively. And the solubility in the five types of oil phases, IPM, liquid paraffin, GTCC, soybean oil, and rapeseed oil are 3.08 ± 0.15 mg/g, 2.27 ± 0.09 mg/g, 1.53 ± 0.08 mg/g, 0.89 ± 0.06 mg/g, and 0.52 ± 0.05 mg/g, respectively. Based on the solubility of CNE, a comparatively greater solubility of CNE was observed in Tween 80, IPM, and propylene glycol. CNE is composed of 0.5% chlorhexidine acetate, 19.2% Tween 80, 4.8% propylene glycol, and 6% IPM. The appearance of CNE is shown in Figure 1A. CHX is a suspension and turbid liquid, but CNE is a clear and transparent solution, as showed in Figure 1A. This result demonstrates that CNE can improve the solubility of chlorhexidine acetate.

Physicochemical characterization of CNE

The CNE nanoemulsion was formed when the liquid became clear. Droplets of CNE appeared dark, and the surrounding liquid appeared bright; thus, a "positive" image was observed using TEM (Figure 1B). Figure 1B demonstrates that the droplet particle sizes were mostly distributed in the 1–100 nm range. Figure 1C shows that the average particle size of CNE was 63.13 nm; 75% of the particles were smaller than 50 nm and 90% of the particles were smaller than 80 nm. In general, the CNE exhibited a relatively restricted size distribution, with PDI values of 0.029, which is less than 0.3. Because the PDI value measures the spread of the particle size distribution, a small PDI value indicates a narrow particle size range.¹³ The zeta potential was -67.13 mV, as shown in Figure 1D. The viscosity, refractive index, and dispersant RI were 0.8872 cP, 1.59 nD₂₀, and 1.330, respectively. These results demonstrate that CNE is stable and fulfills the essential characteristics of CNE.

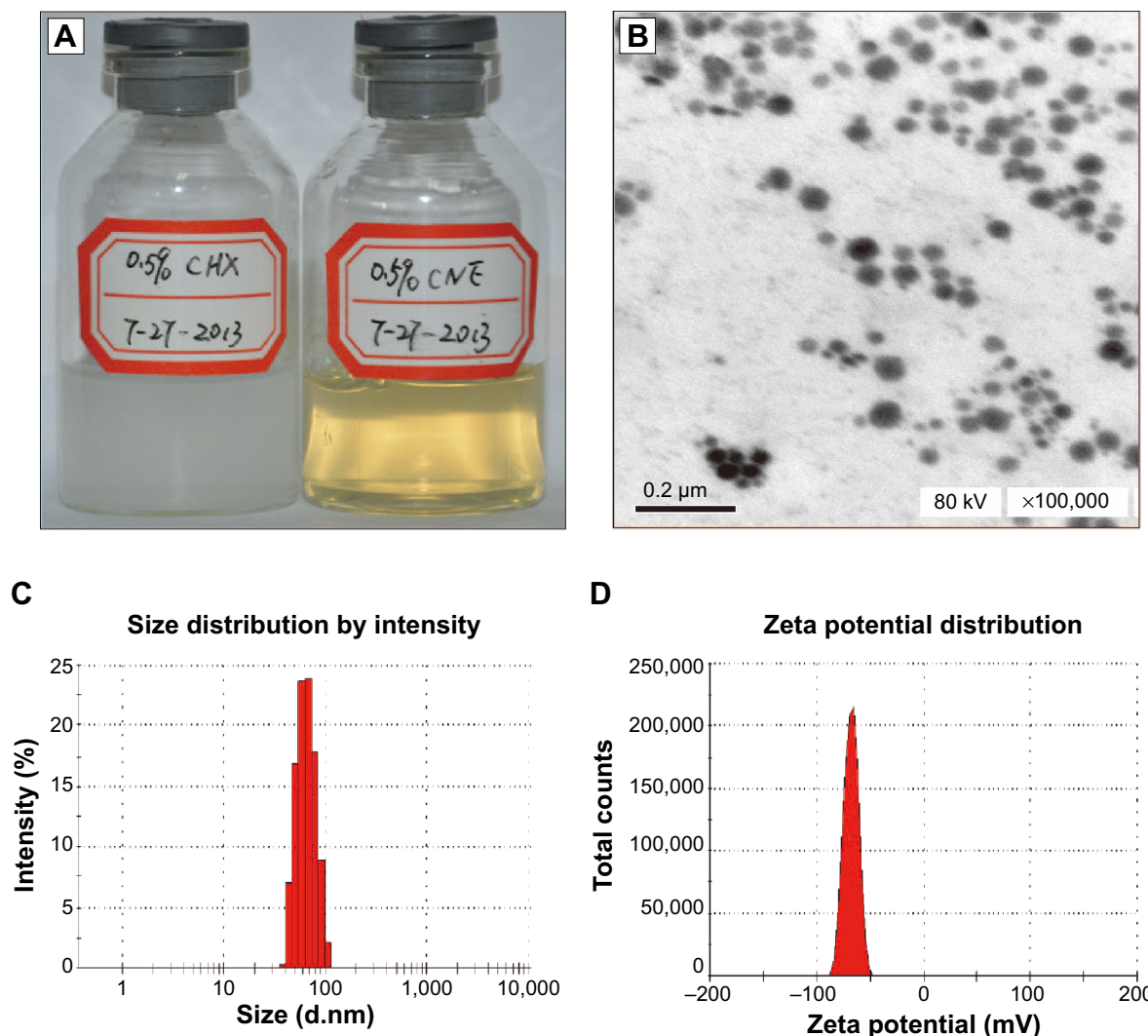


Figure 1 Appearance and physical characteristics of CNE.

Notes: (A) Appearance of 0.5% (5 mg/mL) CHX and 0.5% (5 mg/mL) CNE; (B) transmission electron micrograph of CNE; (C) size distribution of CNE; (D) zeta potential distribution of CNE.

Abbreviations: CNE, chlorhexidine acetate; CHX, chlorhexidine acetate water solution.

Stability evaluation of CNE

CNE exhibits no turbidity, phase separation, precipitation, drug separation, demulsification, and/or creaming after centrifugation at $13,000\times g$ for 30 minutes. This result showed that CNE is very stable.

The stability results of the CNE are shown in Figure 2A–D. The stability of the CNE did not change in observable appearance (flocculation, stratification, precipitation, or creaming and emulsification) either in the natural state or after high-speed centrifugation ($13,000\times g$, 30 minutes). The essential characteristics such as particle size, zeta potential, concentration, and pH did not show any obvious changes when CNE was stored at room temperature for one year (Figure 2A–D). These results have also confirmed

that the nanoemulsion is a thermodynamically stable system with particular concentrations of oil, surfactant, and water, with no phase separation, creaming, or cracking.

In vitro release studies

The in vitro release profile of CNE and CHX resuspension was studied in PBS and artificial saliva as release medium (Figure 3A and B). From Figure 3A and B, it is clear that CHX release is exponentially faster, while CNE release from the drug suspension is slower. In Figure 3A and B, according to in vitro release profiles of CNE and CHX, we find that the accumulative release speed of CNE in PBS was much faster than that in artificial saliva, which could be because the artificial saliva may inhibit the release. Importantly,

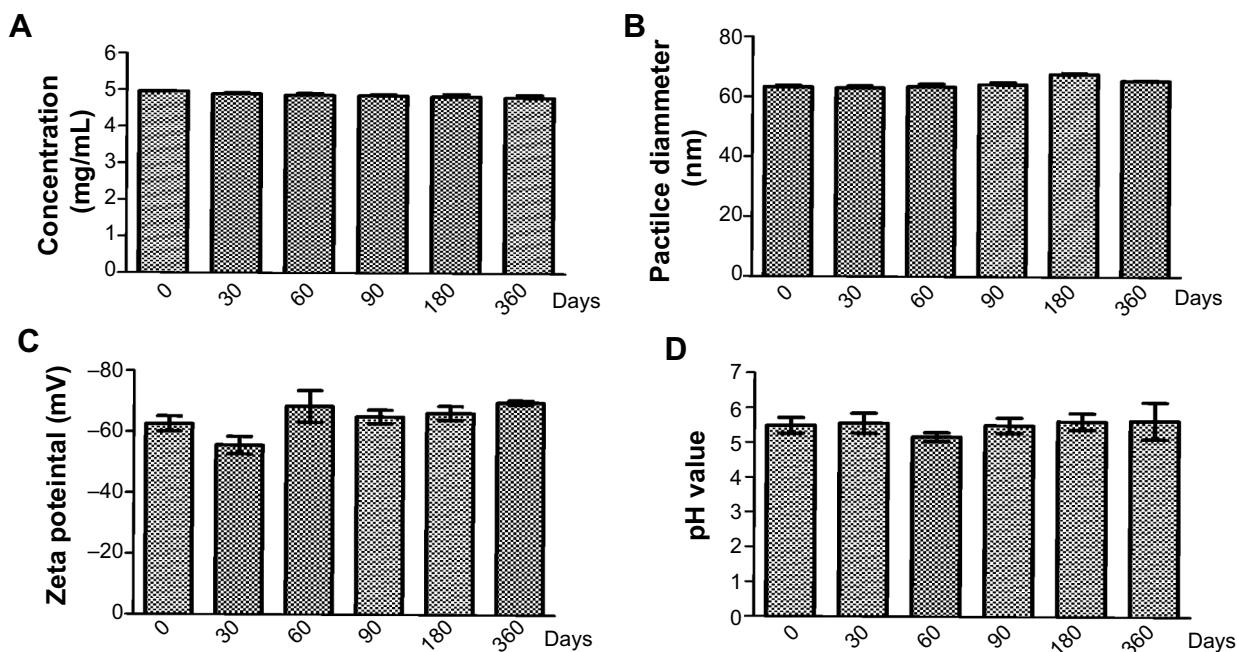


Figure 2 Stability study results of CNE.

Notes: (A) Chlorhexidine acetate concentration change of CNE; (B) size change of CNE; (C) zeta potential change of CNE; (D) pH change of CNE.

Abbreviation: CNE, chlorhexidine acetate.

in both release mediums, the release speed of CHX from nanoemulsions was obviously slower than the suspension (Figure 3A and B). The accumulative release of CHX and CNE in PBS was $90.97\% \pm 0.12\%$ and $35.78\% \pm 0.03\%$, respectively, within 30 minutes, while that in artificial saliva was $69.74\% \pm 0.44\%$ and $20.59\% \pm 0.38\%$, respectively. Also, complete release (100% release rate) times of CNE (3 hours and 6 hours) are 1.5 times and twofold those of CHX (2 hours and 3 hours) in PBS and artificial saliva. In conclusion, the CNE displays sustained-release characteristics, and also have significant difference in vitro release behavior, compared with CHX ($P=0.001$, $P<0.01$; $P=0.002$, $P<0.01$).

Determination of MIC and MBC

The MICs of CNE and CHX are 0.4 and 0.8 $\mu\text{g/mL}$ (Figure 3C and D). The MIC of CHX for *S. mutans* is two times that of CNE. BNE had no obvious antibacterial effect on *S. mutans*. The antibacterial effect of 0.2 and 0.4 $\mu\text{g/mL}$ CNE is significantly different from that of CHX ($P=0.001$, $P<0.01$), as showed in Figure 3C. In addition, 0.4 $\mu\text{g/mL}$ CNE produced a clear effect; however, 0.4 $\mu\text{g/mL}$ CHX failed to inhibit bacterial growth. The MBC of CNE and CHX are 0.4 and 0.8 $\mu\text{g/mL}$, respectively in the Figure 3E. These results demonstrate that CNE exhibits a stronger antibacterial effect than does CHX on *S. mutans* in vivo.

Time-kill assays

Results of time-kill assays of CNE against *S. mutans* are presented in Figure 3F. We observed that the nanoemulsion exhibited a faster and more powerful bactericidal activity than did CHX. The time-kill study of *S. mutans* ATCC 700610 revealed that time- and concentration-dependent killing occurred, with a 95% reduction in bacterial viability within 5 minutes at 0.8 $\mu\text{g/mL}$ CNE and complete killing within 480 minutes (Figure 2D). The time-kill assay revealed that 0.8 $\mu\text{g/mL}$ of CNE exhibited a fast-acting bactericidal efficacy against *S. mutans* (95.07% cell death within 5 minutes), compared with CHX (73.33%) ($P=0.000$, $P<0.01$). In addition, time-kill assays also confirmed that CNE has a stronger antibacterial effect than CHX.

Assay for antimicrobial activity of CNE in vivo

Oral colony number results are shown in Figure 4A. We found that the oral colony numbers decreased with a treatment for 14–28 days. After treatment with 2 mg/mL CNE twice per day for 14 days, the oral colony numbers were significantly lower than those seen with CHX ($P=0.000$, $P<0.01$). In addition, the oral colony numbers with 5 mg/mL CNE also were significantly lower than those with CHX ($P=0.000$, $P<0.01$). Importantly, the oral colony numbers after treatment with 2 and 5 mg/mL CNE were lower than

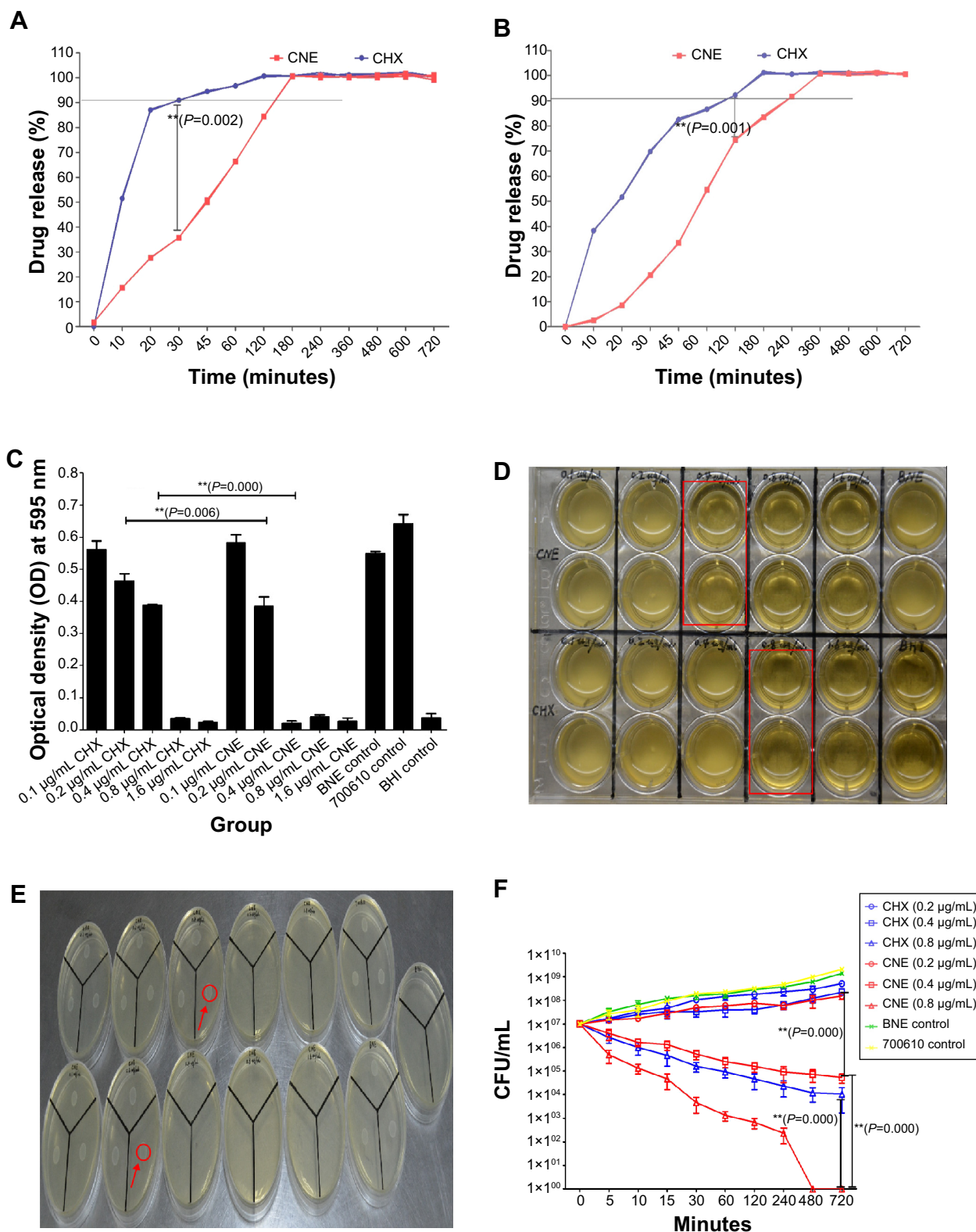


Figure 3 Results of release profile and antibacterial activity against *Streptococcus mutans* in vitro: **(A)** In vitro release profile of CNE and free CHX suspension in PBS as release medium; **(B)** In vitro release profile of CNE and free CHX suspension in artificial saliva as release medium; **(C)** Results of the minimum inhibitory concentrations (MIC) study; **(D)** 24-well plate figure of MIC; **(E)** BHI agar plate of minimum bactericidal concentrations (MBC); **(F)** Results of the time-kill assay.

Note: A black straight line was marked the almost release **(A, B)**. We observed that all *S. mutans* bacteria were killed under the 0.05 absorbance value for the optical density (red line) at 595 nm **(A, B)**. The visibly clear groups of the 24-well plate were marked by red squares **(D)**. Growing white bacterial colonies are indicated with a red circle **(E)**. 700610 means *S. mutans* control. ****** $P < 0.01$ represent a significant difference; ***** $P < 0.05$ represent a difference **(A–C, F)**.

Abbreviations: CNE, chlorhexidine acetate; CHX, chlorhexidine acetate water solution; CFU, colony forming unit; BNE, blank nanoemulsion; BHI, Brain heart infusion; PBS, phosphate buffered saline.

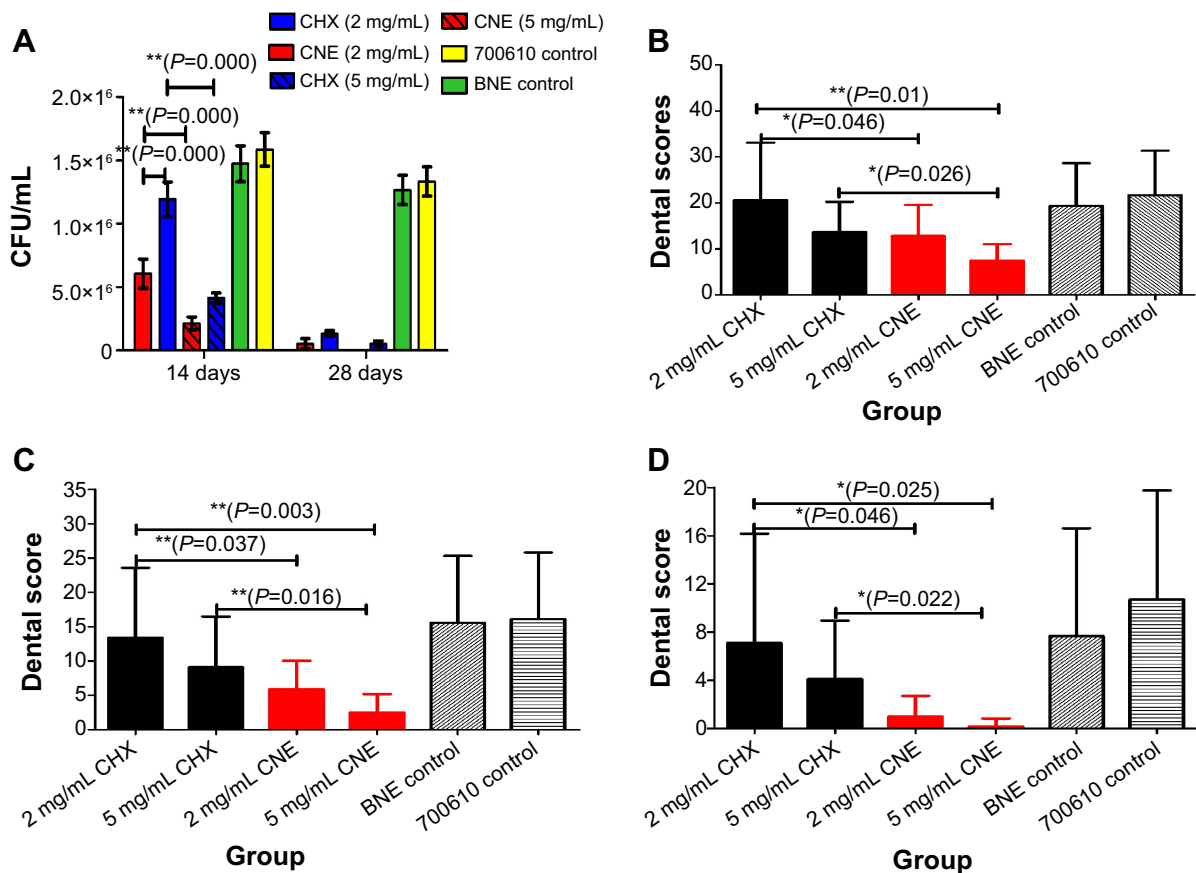


Figure 4 Antibacterial activity and dental score results against *Streptococcus mutans* in vivo: (A) Oral *S. mutans* colony-forming unit results; (B) Dental score results for enamel only; (C) Dental score results for slight dental lesions (Ds); (D) Dental score results for moderate dental lesions (Dm).

Note: 700610 means *S. mutans* control. ** $P < 0.01$ represent a significant difference; * $P < 0.05$ represent a difference.

Abbreviations: CNE, chlorhexidine acetate; CHX, chlorhexidine acetate water solution; BNE, blank nanoemulsion.

those observed after treatment with the same concentration of CHX continuously for 28 days. These data show that CNE has a stronger antibacterial effect than CHX.

Dental score results are shown in Figure 4B–D. We observed that the smooth surface caries scores of all drug-treated animals were significantly lower than those of the BNE and model control groups. Importantly, enamel only scores (S) for 2 mg/mL and 5 mg/mL CNE were obviously lower than those for the same concentration of CHX ($P = 0.046$, $P = 0.025$, $P < 0.05$). In addition, scores decreased with increasing drug concentrations, as shown in Figure 4B. The scores for slight dental lesions (Ds) of the 2 mg/mL and 5 mg/mL CNE group are also obviously lower than those for the same concentration of CHX ($P = 0.037$, $P = 0.016$, $P < 0.05$). Also, slight dental lesion scores of all drug-treated animals were significantly lower than those of the BNE and 700610 model control groups. The slight dental lesion scores for 2 mg/mL and 5 mg/mL CNE were both obviously lower than those for the same concentration of CHX, as showed in Figure 4B and

C. The moderate dental lesion (Dm) scores were similar to the results obtained for enamel caries and slight dental lesions, as showed in Figure 4D. Moderate dental lesions of the 2 mg/mL and 5 mg/mL CNE groups were both significantly lower than those of the same concentration of CHX ($P = 0.046$, $P = 0.022$, $P < 0.05$).

The representative photographs of animal teeth are as follows: Figure 5A, treated with 2 mg/mL CHX water solution; Figure 5B, treated with 5 mg/mL CHX water suspension; Figure 5C, treated with 2 mg/mL CNE; Figure 5D, treated with 5 mg/mL CNE; Figure 5E, treated with BNE; Figure 5F, 700610 model control. Different colors axes are marked in Figure 5A–F. Green arrows indicate enamel only dental lesions; the blue arrows indicate slight dental lesions; the red arrows indicate moderate dental lesions. We observed that the teeth of the 2 mg/mL CHX group exhibited moderate dental lesions and slight dental lesions, as shown in Figure 5A, and that the teeth of the 5 mg/mL CHX group exhibited enamel only dental lesions and slight dental lesions, as shown in Figure 5B. Also the teeth

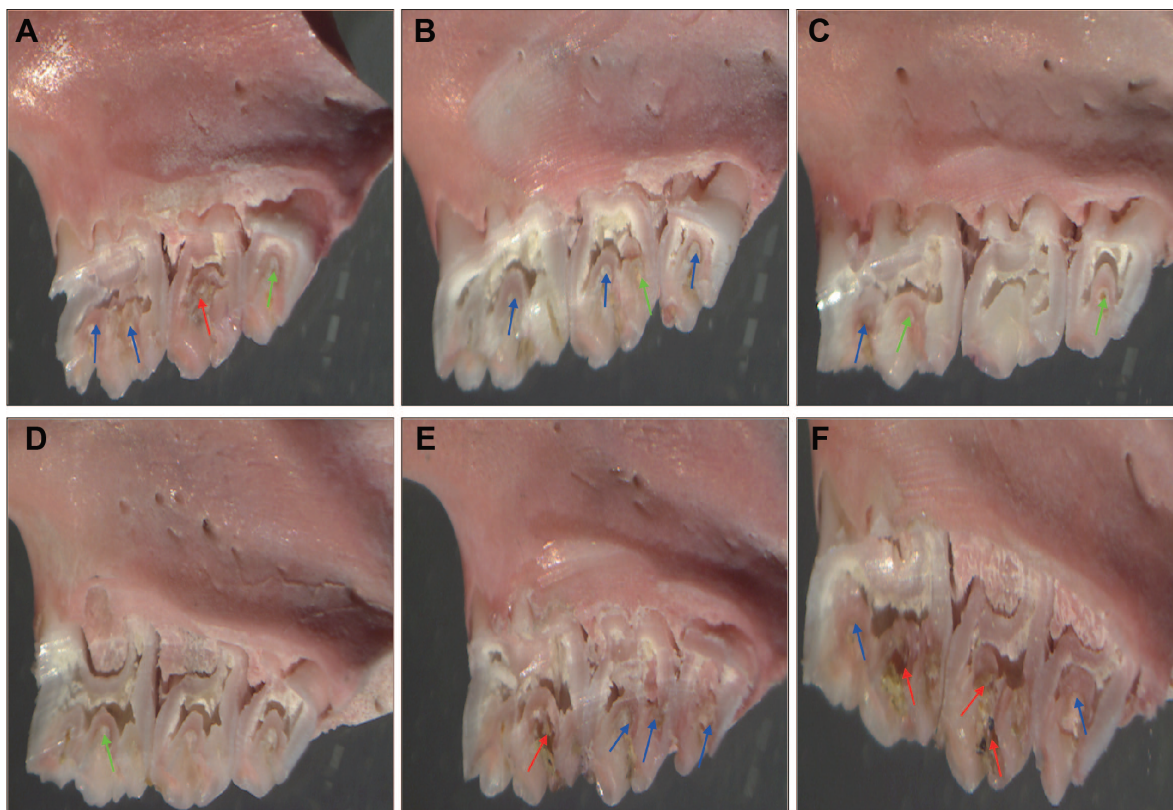


Figure 5 Photos of teeth with dental caries: treated with a 2 mg/mL CHX water solution (A); treated with a 5 mg/mL CHX water suspension (B); treated with 2 mg/mL CNE (C); treated with 5 mg/mL CNE (D); treated with BNE (E); 700610 control (F).

Note: 700610 means *Streptococcus mutans* control. These photos were taken using a stereo microscope at the original magnification (10×23 times). Green arrows indicate enamel only dental lesions; the blue arrows indicate slight dental lesions; the red arrows indicate moderate dental lesions.

Abbreviations: CNE, chlorhexidine acetate; CHX, chlorhexidine acetate water solution; BNE, blank nanoemulsion.

of the 2 mg/mL CNE group exhibited enamel only dental lesions and slight dental lesions, as shown in Figure 5C, and the teeth of the 5 mg/mL CNE group exhibited enamel only dental lesions, as shown in Figure 5D. The teeth of the BNE and 700610 model groups both exhibited moderate dental lesions and slight dental lesions, as shown in Figure 5E and F. In general, for all animals treated with 2 mg/mL and 5 mg/mL CNE, the scores of enamel only dental lesion, slight dental lesions, and moderate dental lesions were significantly lower than those with the same concentration of CHX and the control group. Importantly, oral colony numbers of animals treated with 2 mg/mL and 5 mg/mL CNE were similar to the scores. Therefore, these results confirm that CNE can improve the antibacterial effect of this drug and reduce dental caries scores.

Inhibition of biofilm formations by CNE

Biofilm formation quantification results for CNE are shown in Figure 6A. We observed that the biofilm formation after CNE treatment is approximately half that after treatment with the same concentration CHX (OD 595 nm, 0.27 ± 0.025 and 0.45 ± 0.022 ,

respectively). This result demonstrates that CNE has a stronger ability to inhibit the biofilm formation of *S. mutans* than does the same concentration of CHX ($P=0.001$, $P<0.01$).

The formation of biofilm surface structure by *S. mutans* is shown in Figure 6B–E. At 2,000× magnification, we observed that the density and amount of *S. mutans* cells after CNE treatment were significantly lower than those observed after treatment with CHX, as showed in Figure 6B and C. At 6,000× magnification, the density and amount of *S. mutans* cells after CNE treatment were also significantly lower than those observed with CHX (Figure 6D and E). In Figure 6E, control *S. mutans* cells with CHX treatment exhibited a short normal rod shape with a smooth, regular surface. *S. mutans* treated with CNE lost their original shape and exhibited a distorted, irregular shape (Figure 6D). When subjected to a combination of CNE, some cells fell to pieces, but cells with a normal shape remained detectable in each field (Figure 6D and E). These results also demonstrate that CNE has a stronger ability to inhibit the biofilm formation of *S. mutans* than does the same concentration of CHX.

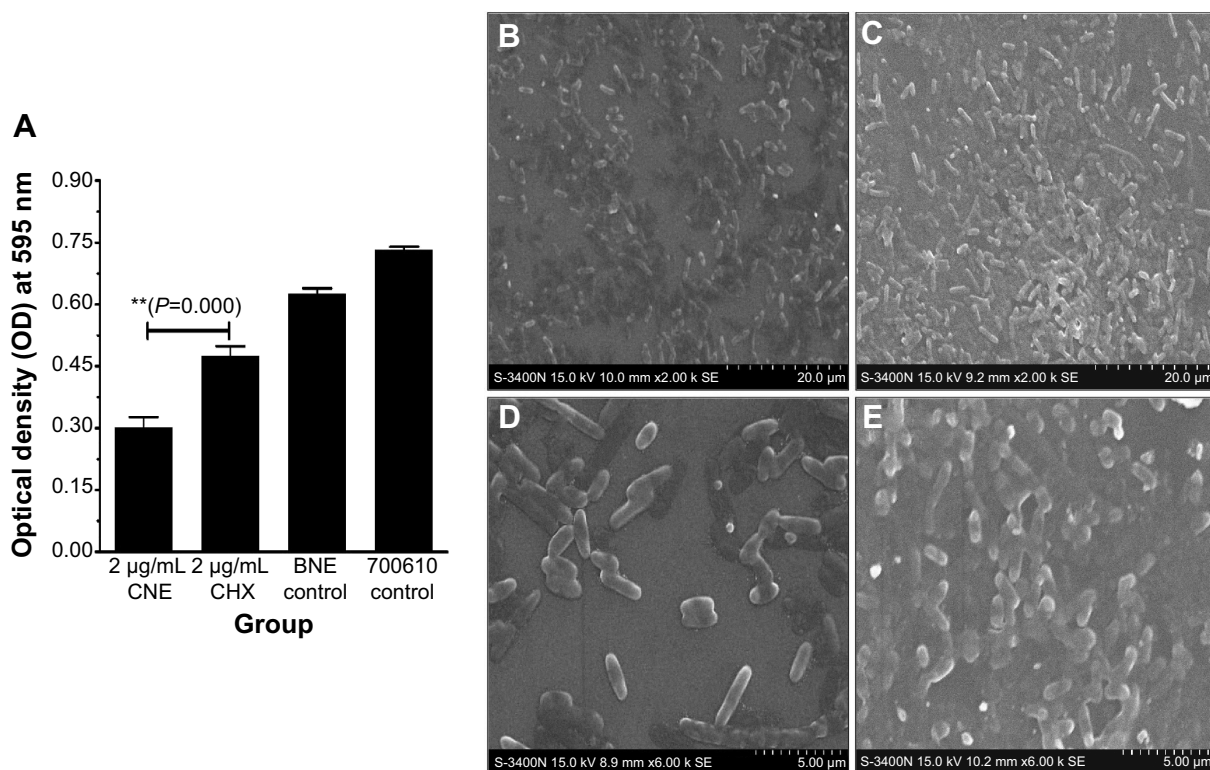


Figure 6 Inhibition of biofilm formation and biofilm surface structure figure: biofilm formation inhibition results for CNE (A); biofilm surface structure after CNE treatment ($\times 2,000$ times) (B); biofilm surface structure after CHX treatment ($\times 2,000$ times) (C); Biofilm surface structure after CNE treatment ($\times 6,000$ times) (D); Biofilm surface structure after CHX treatment ($\times 6,000$ times) (E).

Notes: 700610 means *Streptococcus mutans* control. $**P < 0.01$ represent a significant difference; $*P < 0.05$ represent a difference.

Abbreviations: CNE, chlorhexidine acetate; CHX, chlorhexidine acetate water solution; BNE, blank nanoemulsion.

The formation of three-dimensional biofilm structures is presented in Figure 7A–D. Topographic and deflection images were generated simultaneously. The data were taken for three profile parameters R_a , R_z , and R_q , and the two measure parameters R_{sk} and R_{ku} . The characteristics of the surfaces were examined in terms of average height and surface roughness. The average height is the mean value of the surface relative to the difference in height between the highest and lowest points on the surface from the median plane. In the gray scale figure, the surface height in the CHX group (Figure 7C) is higher than that in the group treated with the same concentration of CNE (Figure 7A). In the color figure, the surface roughness in the CHX group (Figure 7D) is stronger than that in the group treated with the same concentration of CNE (Figure 7B). The profile parameter and measure parameter results are presented in Figure 7E and F, respectively. The R_a , R_q , R_z , R_{sk} (Ratio), and R_{ku} (Ratio) of the CHX group were 105.30 ± 25.39 nm, 486.84 ± 103.43 nm, 125.70 ± 29.69 nm, 1.43 ± 0.09 , and 2.31 ± 0.41 , respectively. The R_a , R_q , R_z , R_{sk} (Ratio), and R_{ku} (Ratio) values of the CNE group were 60.64 ± 19.23 nm, 331.24 ± 95.05 nm, 73.36 ± 24.01 nm, 1.52 ± 0.20 , and 2.82 ± 0.99 , respectively. The profile parameters R_a , R_z , and R_q

after $0.2 \mu\text{g/mL}$ CNE treatment were all higher than those after CHX treatment. The R_a , R_q , R_z of the CHX group were 1.73, 1.46, and 1.71 times those of the CNE group. Nonetheless, the results of the measurement parameters R_{ku} and R_{sk} were reversed. These results also confirm that CNE has a stronger ability to inhibit the biofilm formation of *S. mutans* than does the same concentration of CHX.

The cell membrane damage of CNE

Cell membrane damage of *S. mutans*, as indicated by TEM, is shown in Figure 8A–D. At $39,000\times$ magnification more obvious holes were observed on the surface of *S. mutans* after treatment with CNE (Figure 8A) than after treatment with CHX (Figure 8B). At $93,000\times$ magnification, the control for CHX revealed relatively intact and clearly discernible cell membranes with uniformly distributed cytochylema (Figure 8D). However, the cells treated with CNE for 48 hours exhibited altered and disrupted cell membranes, as depicted in Figure 7C. The cytoplasmic membrane appeared to be locally separated from the cell envelope. Some cells after CNE treatment were irregularly shaped, and parts of the cell wall were broken; this process may result in the leakage

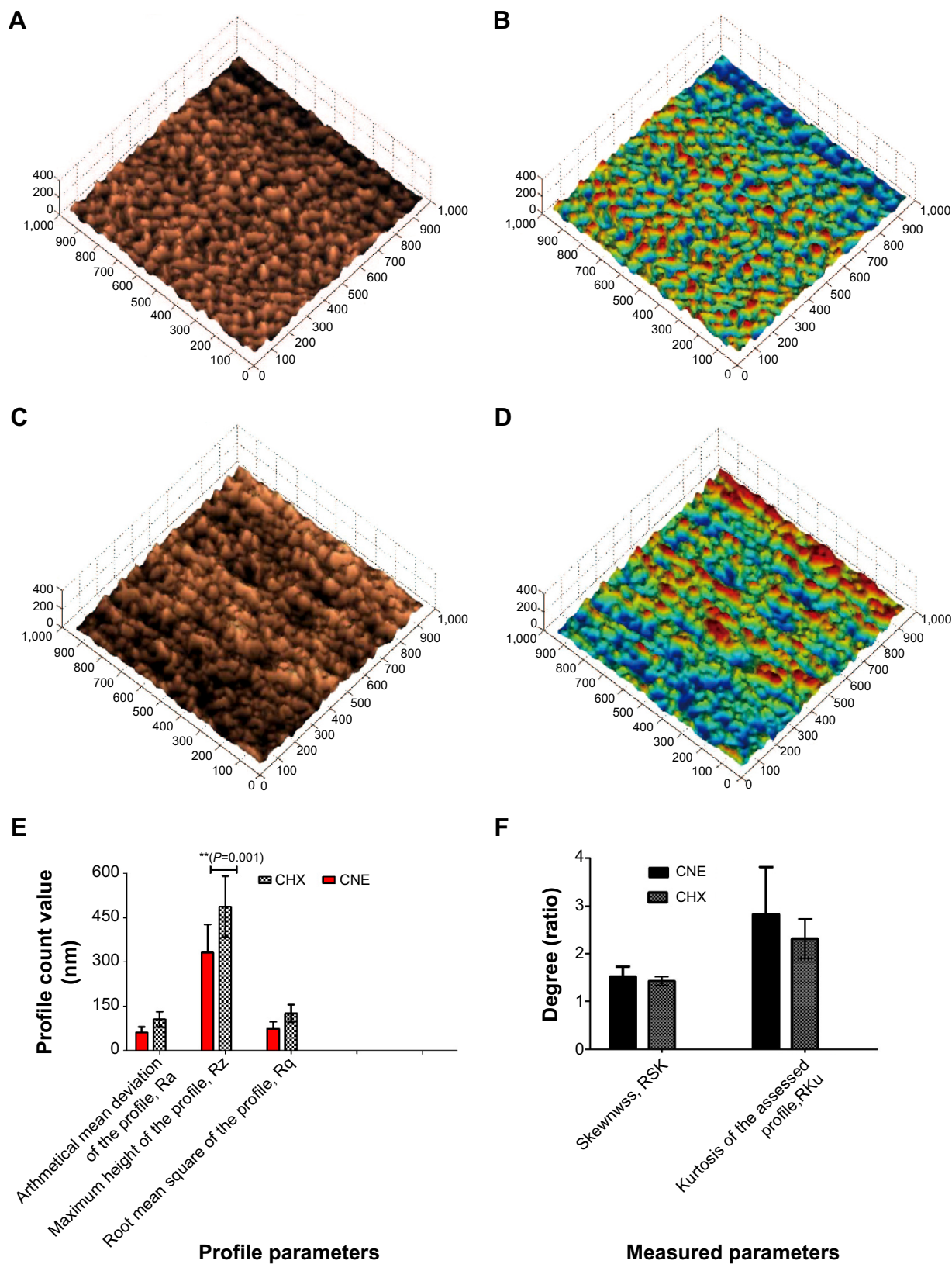


Figure 7 Three-dimensional surface structure figure of biofilm by AFM; **(A)** gray scale figure of biofilm morphology after treatment with 0.2 $\mu\text{g/mL}$ CNE; **(B)** color figure of biofilm morphology after treatment with 0.2 $\mu\text{g/mL}$ CNE; **(C)** gray scale figure of biofilm morphology after treatment with 0.2 $\mu\text{g/mL}$ CHX; **(D)** color figure of biofilm morphology after treatment with 0.2 $\mu\text{g/mL}$ CNE; **(E)** profile parameter results; **(F)** measure parameters results.

Note: $**P < 0.01$ represent a significant difference; $*P < 0.05$ represent a difference.
Abbreviations: CNE, chlorhexidine acetate; CHX, chlorhexidine acetate water solution.

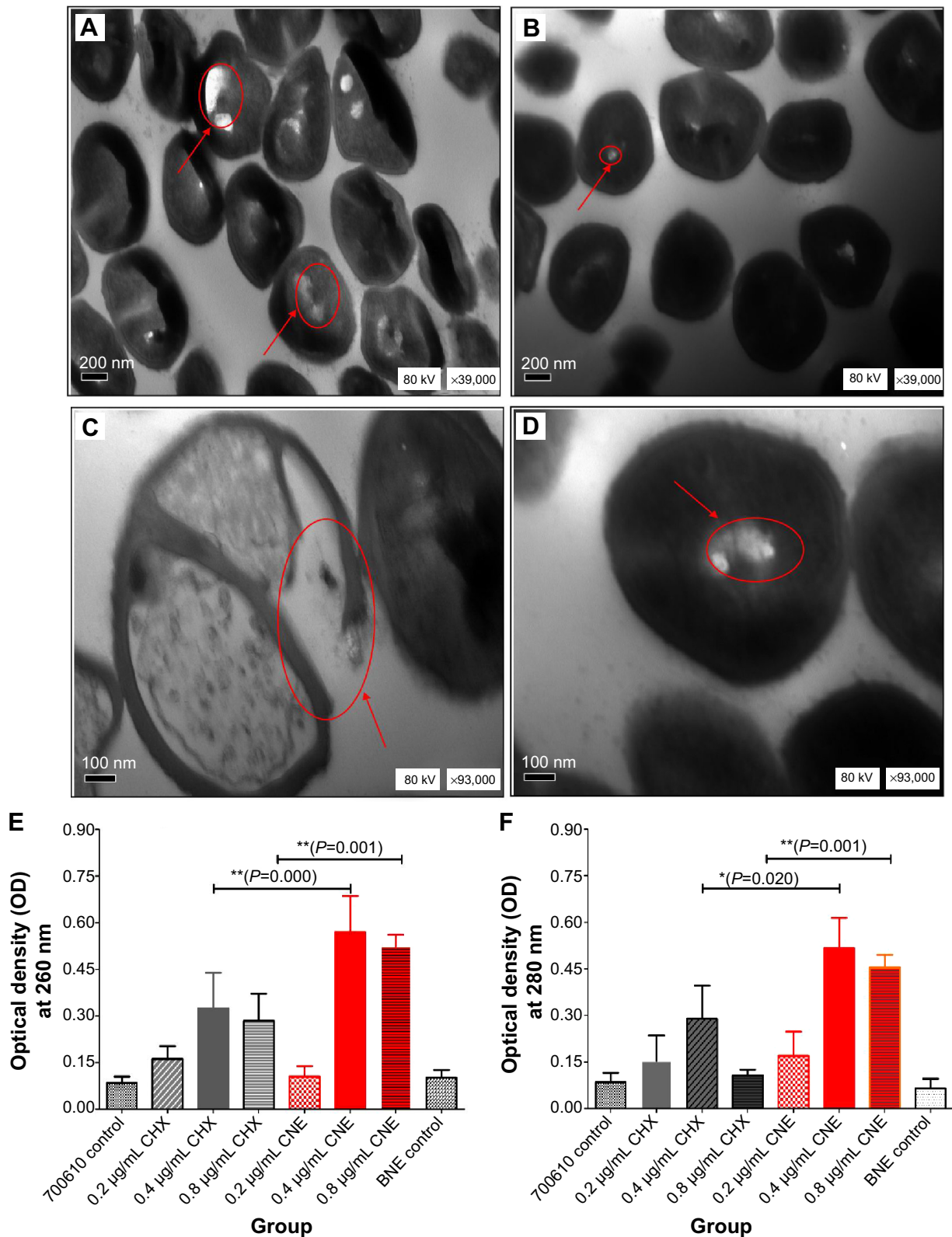


Figure 8 Cell membrane structural damage and cell membrane integrity results; (A) cell membrane structural damage after treatment with 0.2 µg/mL CNE (×39,000 times); (B) cell membrane structural damage after treatment with 0.2 µg/mL CHX (×39,000 times); (C) cell membrane structural damage after treatment with 0.2 µg/mL CNE (×93,000 times); (D) cell membrane structural damage after treatment with 0.2 µg/mL CHX (×93,000 times); (E) leaking DNA concentration of *Streptococcus mutans* treated CNE; (F) leaking protein concentration of *S. mutans* treated CNE.

Notes: Cell membrane structural damage was remarked with red and arrowed circle. 700610 means *S. mutans* control. ** $P < 0.01$ represents a significant difference; * $P < 0.05$ represents a difference.

Abbreviations: CNE, chlorhexidine acetate; CHX, chlorhexidine acetate water solution; BNE, blank nanoemulsion.

of nutrients and nucleic materials. The extent of this breakage was severe, compared with that observed after treatment with CHX (Figure 8C and D). The cell membrane disruption was more severe in the 0.2 µg/mL CNE group than in the CHX group. These results demonstrated that CNE exhibits a stronger ability to damage the cell membrane structure of *S. mutans* than does the same concentration of CHX.

Cell membrane integrity results are shown in the Figure 8E and F. In Figure 8E, The OD 260 nm values of *S. mutans* treated with 0.4 and 0.8 µg/mL CNE are both significantly higher than those obtained with the same concentrations of CHX ($P=0.000$, $P=0.001$, $P<0.01$). These results indicate that the leaking DNA concentrations of *S. mutans* treated with 0.4 and 0.8 µg/mL of CNE are both higher than those observed with the same concentration of CHX, due to cell membrane damage. In Figure 8F, the OD 280 nm values of *S. mutans* treated with 0.4 and 0.8 µg/mL of CNE are both higher than those obtained with the same concentration of CHX ($P=0.001$, $P=0.020$). These results indicate that the leaking protein concentrations of *S. mutans* treated with 0.4 and 0.8 µg/mL of CNE are both higher than those observed with the same concentration of CHX, due to cell membrane damage. In addition, the OD at 260 and 280 nm after treatment with 0.4 and 0.8 µg/mL CNE are 1.75 and 1.78 times and 6.25 and 4.43 times those obtained with CHX, respectively, in the cell membrane integrity test. These results demonstrated that CNE exhibits a stronger ability to damage the cell membrane integrity of *S. mutans* than does the same concentration of CHX.

Discussion

Despite all efforts toward control and prevention, dental caries remain a global health problem affecting all ages. *S. mutans* growth is an essential process in dental caries development.¹⁶ Moreover, *S. mutans* plays a key role in the development of oral biofilms through the production of extracellular polysaccharides. *S. mutans* is a major target for the prevention of dental caries; thus, we chose *S. mutans* as an antibacterial objective in our research. CNE is the most researched and most recommended agent for use in the oral cavity.²⁰ This agent is effective against bacteria that are widely found in the oral cavity and against organisms associated with diseases of the oral cavity. Despite their significant in vitro antimicrobial activity against cariogenic microorganisms, the routine use of antiseptics is not advisable due to poor water solubility and local side effects, such as soreness of the oral mucosa, irritation of taste buds, and discoloration of the teeth, tongue, restorations, and dentures. It is necessary to improve the water solubility of CNE.

The application of nanoemulsions as antimicrobial agents is a new and promising innovation.⁸ Many studies have demonstrated the antimicrobial properties of nanoemulsions formulated with antimicrobial substances.²¹ Investigations on the use of nanoemulsions as antimicrobial agents were prompted by the development of antimicrobial-resistant strains after the use of existing agents, due to the widespread and sometimes inappropriate use of antibiotics, disinfectants, and antiseptics. Moreover, nanoemulsions are novel water-in-oil formulations that are stabilized by adding small amounts of surfactants. Importantly, nanoemulsions can significantly enhance the solubility of poorly water-soluble drugs to improve bioavailability. We aimed to improve the solubility and bioavailability of this agent using a nanoemulsion. The results demonstrated that this novel CNE has a fast-acting bactericidal efficacy against *S. mutans* in vivo and in vitro. Also, these results confirmed that nanoemulsions have extensive bactericidal, sporicidal,²² and virucidal effects.²³ It is important to determine the mechanism by which CNE can enhance the antibacterial effect of this agent against dental caries during *S. mutans* infection.

Biofilms play a causative role and are formed by microorganisms on the teeth and gums surface of dental caries. Biofilm formation is accomplished via the attachment, detachment, and accumulation of oral microbial flora on the tooth surface. Importantly, three-dimensional structures are present in the oral cavity, consisting of bacterial strains anchored to solid surfaces such as tooth enamel, tooth roots, or dental implants.¹⁹ Thus, we considered the antibacterial effect of CNE on the inhibition of biofilms in vivo. The results demonstrated that biofilm formation after 0.2 µg/mL CNE treatment is roughly half of what is seen after treatment with its water solution (0.27/0.45, OD 595 nm). These results were further confirmed using SEM and AFM. The results suggest that the ability of nanoemulsions loaded with CNE to inhibit biofilm formation is stronger than that of the same concentration of CHX.

It was also important to determine whether CNE acted on the cell membrane of *S. mutans*. We found that the mechanism of action of the nanoemulsion appears to be nonspecific disruption of bacterial cell membranes.⁸ The antibacterial action of CNE also targets the bacterial cell membrane.²⁴ Therefore, the ability of CNE to damage the cellular membrane structure of *S. mutans* was also examined. The TEM results demonstrated that CNE exhibits a stronger ability to damage the cellular membrane structure of *S. mutans* than does the same concentration of CHX. In addition, the OD values at 260 and 280 nm after treatment with 0.4 and

0.8 µg/mL CNE were 1.75 and 1.78 times and 6.25 and 4.43 times those obtained after treatment with CHX, in the cell membrane integrity test.

In summary, these results demonstrated that a novel nanoemulsion loaded with poorly water-soluble CNE improved the aqueous solubility and the antimicrobial activity of this agent against *S. mutans* in vitro and in vivo by inhibiting effective biofilm formation and enhancing damage to the structure and integrity of the cell membrane.

However, the essential process of dental caries formation involves bacterial adherence to tooth surfaces, dental plaque formation, and localized demineralization of tooth enamel by acids of bacterial origin.²⁵ In addition, evidence indicates that *S. mutans* and *Streptococcus sobrinus* play a central role in the pathogenesis of this disease.²⁶ In our previous study, the MICs of CNE were 0.1 µg/mL and 0.2 µg/mL for two clinical strains of *S. mutans* isolated from Southwest Hospital; however, the equivalent values for CHX were both 0.8 µg/mL. CNE is more effective against *S. mutans*, but *S. sobrinus* must be studied further. Further, dental caries are very complex. In our study, we examined biofilms as a key factor, but it would be useful to study the effect of CNE on additional factors. We also studied other factors, such as adherence ability, acid production, and extracellular polysaccharide production. These data demonstrate that CNE exhibits better activity than CHX. However, these studies included no normal standard and generated some defective results. Hence, we did not report these results. Many areas, such as participant administration and oral drug kinetics of CNE, must be studied further. Safety of novel nanoemulsions is very important. Consecutive treatment twice per day for 28 days caused no obvious toxicity, such as death or bleeding. Also, we chose the highest content CNE (5 mg/mL) act on the standard cell toxicity cell L929 line act for 48 hours. The cell survival ratio with CNE is 87.29%±0.01% (belongs to grade 1, low toxicity), according to ISO 10993-5:1999 (Part 5: Tests for in vitro cytotoxicity standard). This result is the same as that of CHX (oral, mice, LD₅₀ (half lethal dose) 2,000 mg/kg, belongs to third grade, low toxicity) in the GB/T 21757-2008 (Acute oral toxicity classification for Chemicals). However, more toxicity studies are required before CNE can be marketed and applied for oral dental caries. These results demonstrate that a novel nanoemulsion loaded with CNE is a promising agent for effectively preventing and curing dental caries.

Conclusion

In this study, a novel CNE nanoemulsion with an average size of 63.13 nm and a zeta potential of -67.13 mV that is composed of 0.5% CNE, 19.2% Tween 80, 4.8% propylene

glycol, and 6% IPM was prepared using the phase inversion method and the pseudoternary phase diagram. Importantly, characteristics such as drug content, size, potential, and pH value of CNE showed no obvious change when stored at room temperature for 1 year. Also, compared with CHX, the release profile results show that CNE has a visibly delayed release effect in both PBS and artificial saliva solutions. With respect to MIC, the data demonstrated that the MBC for CHX against *S. mutans* is two times that of CNE. The time-kill assay also demonstrated that 0.8 µg/mL CNE (95.07%) has a fast-acting and better bactericidal efficacy than CHX (73.33%). In in vivo tests, for all animals treated with 2 mg/mL and 5 mg/mL CNE, the scores for enamel only dental lesions, slight dentinal lesions, and moderate dentinal lesions were significantly lower than those observed for the same concentration of CHX and the control group. The oral colony numbers obtained for 2 mg/mL and 5 mg/mL CNE were similar to the score results. CNE treatment at a concentration of 0.2 µg/mL inhibited biofilm formation more effectively than CHX, as indicated by the crystal violet staining method, SEM, and AFM. The cell membrane of *S. mutans* was also severely disrupted by 0.2 µg/mL CNE, as indicated by TEM. These results indicated that the leaking DNA and protein amounts of *S. mutans* treated with 0.4 and 0.8 µg/mL of CNE were both higher than those observed with the same concentration of CHX, due to cell membrane damage. These results also demonstrated that a novel nanoemulsion loaded with poorly water-soluble CNE improved the aqueous solubility and the antimicrobial activity of this agent against *S. mutans* in vitro and in vivo by inhibiting effective biofilm formation and enhancing damage to the structure and integrity of the cell membrane. We hope this novel nanoemulsion is a promising medicine for preventing and curing dental caries.

Acknowledgments

This work was supported by National Key Technology R&D Program (Number 2014BAI15B00/2014BAI15B01), Natural Science Foundation Project of CQ CSTC (Number 20142014jcyjA10107), and College Students' Innovative Undertaking Plan Project of Third Military Medical University of PLA (Number 201390035037). We are also grateful to Drs Zhonglin Chen and Jianchun Yang from the Department of Stomatology of First Affiliated Hospital (Southwest Hospital), Third Military Medical University of PLA, for evaluating the dental caries using the Keyes methods (1958).

Disclosure

The authors report no conflicts of interest in this work.

References

- Zander A, Sivanewaran S, Skinner J, Byun R, Jalaludin B. Risk factors for dental caries in small rural and regional Australian communities. *Rural Remote Health*. 2013;13(3):2492.
- Shakeri R, Malekzadeh R, Etemadi A, et al. Association of tooth loss and oral hygiene with risk of gastric adenocarcinoma. *Cancer Prev Res (Phila)*. 2013;6(5):477–482.
- Prasai Dixit L, Shakya A, Shrestha M, Shrestha A. Dental caries prevalence, oral health knowledge and practice among indigenous Chepang school children of Nepal. *BMC Oral Health*. 2013;13(20):5.
- Liu L, Zhang Y, Wu W, Cheng M, Li Y, Cheng R. prevalence and correlates of dental caries in an elderly population in northeast China. *PLoS One*. 2013;8(11):e78723.
- Wu L, Chang R, Mu Y, et al. Association between obesity and dental caries in Chinese children. *Caries Res*. 2013;47(2):171–176.
- Bagramian RA, Garcia-Godoy F, Volpe AR. The global increase in dental caries. A pending public health crisis. *Am J Dent*. 2009;22(1):3–8.
- Tong Z, Tao R, Jiang W, et al. In vitro study of the properties of Streptococcus mutans in starvation conditions. *Arch Oral Biol*. 2011;56(11):1306–1311.
- Karthikeyan R, Amaechi BT, Rawls HR, Lee VA. Antimicrobial activity of nanoemulsion on cariogenic Streptococcus mutans. *Arch Oral Biol*. 2011;56(5):437–445.
- Autio-Gold J. The role of chlorhexidine in caries prevention. *Oper Dent*. 2008;33(6):710–716.
- Sajjan PG, Nagesh L, Sajjanar M, Reddy SK, Venkatesh UG. Comparative evaluation of chlorhexidine varnish and fluoride varnish on plaque Streptococcus mutans count – an in vivo study. *Intl Jf Dent Hyg*. 2013; 11(3):191–197.
- Riggs PD, Braden M, Patel M. Chlorhexidine release from room temperature polymerising methacrylate systems. *Biomaterials*. 2000;21(4): 345–351.
- Musa SH, Basri M, Masoumi HR, et al. Formulation optimization of palm kernel oil esters nanoemulsion-loaded with chloramphenicol suitable for meningitis treatment. *Colloids Surf B Biointerfaces*. 2013;112:113–119.
- Sun H, Liu K, Liu W, et al. Development and characterization of a novel nanoemulsion drug-delivery system for potential application in oral delivery of protein drugs. *Int J Nanomed*. 2012;7:5529–5543.
- Zhao L, Wei Y, Huang Y, He B, Zhou Y, Fu J. Nanoemulsion improves the oral bioavailability of baicalin in rats: in vitro and in vivo evaluation. *Int J Nanomedicine*. 2013;8:3769–3779.
- Gil FJ, Sanchez LA, Espias A, Planell JA. In vitro corrosion behaviour and metallic ion release of different prosthodontic alloys. *Int Dent J*. 1999;49(6):361–367.
- Fu D, Pei D, Huang C, Liu Y, Du X, Sun H. Effect of desensitising paste containing 8% arginine and calcium carbonate on biofilm formation of Streptococcus mutans in vitro. *J Dent*. 2013;41(7):619–627.
- Keyes PH. Dental caries in the molar teeth of rats. I. Distribution of lesions induced by high-carbohydrate low-fat diets. *J Dent Res*. 1958;37(6):1077–1087.
- Keyes PH. Dental caries in the molar teeth of rats. II. A method for diagnosing and scoring several types of lesions simultaneously. *J Dent Res*. 1958;37(6):1088–1099.
- Krzysciak W, Jurczak A, Koscielniak D, Bystrowska B, Skalniak A. The virulence of Streptococcus mutans and the ability to form biofilms. *Eur J Clin Microbiol Infect Dis*. 2013;33(4):499–515.
- Arslan S, Silici S, Perçin D, Koç AN, Er O. Antimicrobial activity of poplar propolis on mutans streptococci and caries development in rats. *Turk J Biol*. 2012;36(3):65–73.
- Hwang YY, Ramalingam K, Bienek DR, Lee V, You T, Alvarez R. Antimicrobial activity of nanoemulsion in combination with cetylpyridinium chloride in multidrug-resistant Acinetobacter baumannii. *Antimicrob Agents Chemother*. 2013;57(8):3568–3575.
- Chepurnov AA, Bakulina LF, Dadaeva AA, Ustinova EN, Chepurnova TS, Baker JR Jr. Inactivation of Ebola virus with a surfactant nanoemulsion. *Acta Trop*. 2003;87(3):315–320.
- Hamouda T, Hayes MM, Cao Z, et al. A novel surfactant nanoemulsion with broad-spectrum sporicidal activity against Bacillus species. *J Infect Dis*. 1999;180(6):1939–1949.
- Van Oosten B, Marquardt D, Komljenovic I, Bradshaw JP, Sternin E, Harroun TA. Small molecule interaction with lipid bilayers: a molecular dynamics study of chlorhexidine. *J Mol Graph Model*. 2014;48:96–104.
- Song JH, Yang TC, Chang KW, Han SK, Yi HK, Jeon JG. In vitro anti-cariogenic activity of dichloromethane fraction from Rheum undulatum L. root. *Arch Pharm Res*. 2006;29(6):490–496.
- Ban SH, Kwon YR, Pandit S, Lee YS, Yi HK, Jeon JG. Effects of a bio-assay guided fraction from Polygonum cuspidatum root on the viability, acid production and glucosyltransferase of mutans streptococci. *Fitoterapia*. 2010;81(1):30–34.

International Journal of Nanomedicine

Publish your work in this journal

The International Journal of Nanomedicine is an international, peer-reviewed journal focusing on the application of nanotechnology in diagnostics, therapeutics, and drug delivery systems throughout the biomedical field. This journal is indexed on PubMed Central, MedLine, CAS, SciSearch®, Current Contents®/Clinical Medicine,

Submit your manuscript here: <http://www.dovepress.com/international-journal-of-nanomedicine-journal>

Dovepress

Journal Citation Reports/Science Edition, EMBASE, Scopus and the Elsevier Bibliographic databases. The manuscript management system is completely online and includes a very quick and fair peer-review system, which is all easy to use. Visit <http://www.dovepress.com/testimonials.php> to read real quotes from published authors.